Fibrillar Morphology of Elastomer-Modified Polypropylene: Effect of Interface Adhesion and Processing Conditions

Ling Zhang,[1] Rui Huang,[1] Gang Wang,[1] Liangbin Li,[2] Haiying Ni,[1] Xinyuan Zhang[3]

[1]*Department of Polymer Materials Science and Engineering, Sichuan University, Chengdu Sichuan 610065, People's Republic of China*
[2]*FOM-Institute of Atomic and Molecular Physics, Kruislaan 407, 1098 SJ Amsterdam, the Netherlands*
[3]*Center of Measurement and Analysis, Sichuan University, Chengdu Sichuan 610065, People's Republic of China*

Received 11 July 2001; accepted 13 February 2002

ABSTRACT: The effect of interface interaction and processing conditions combined with the viscosity ratio of elastomer domains to the polypropylene (PP) matrix (η_d/η_m, subscript *d* and *m* designate the dispersed phase and the matrix, respectively) on fibril formation was investigated. A close to unity viscosity ratio, high interface interaction between the two phases, and a high shear rate in molding were found to result in fibril dispersion. A low-viscosity elastomer tended to form fibrils also. A high extrusion shear rate seems to have no effect on fibrillar formation, but the dispersion size (D_n) decreased from 0.25 to 0.19 μm with an increasing screw speed from 120 to 160 rpm. The Izod impact strength of blends appears to be optimum when a fine and uniform and nonfibril morphology of the elastomer in PP is formed. © 2002 Wiley Periodicals, Inc. J Appl Polym Sci 86: 2085–2092, 2002

Key words: poly(propylene) (PP); elastomers; interfaces; morphology; toughness

INTRODUCTION

An improvement of toughness is of particular interest, since the toughness of polymeric materials is an important selection criterion for many applications. Toughness generally reflects the degree of energy absorption from the beginning of the mechanical load to the final fracture. However, toughness is one of the most complex properties and is difficult to control, because it is greatly influenced by many morphological and micromechanical parameters.[1] Therefore, it is of fundamental importance to understand the relationship between the morphology and the properties of polymers for the development of polymer systems with improved toughness. In recent years, use of elastomers as impact modifiers of polymers is well documented in the literature. Blends of polypropylene (PP) with various impact modifiers have been investigated in the literature, such as, ethylene–propylene rubber (EPR),[2] ethylene–propylene–diene rubber (EPDM),[3] ethylene–hexene rubber,[4] and styrene–ethylene butylene–styrene rubber (SEBS).[5,6] A recent addition to the family of the thermoplastic elastomer is the ethylene–octene copolymer (EOC), which is catalyzed by homogeneous metallocene catalysts.

In immiscible polymer blends, the properties greatly depend on the morphology, which is basically determined by the following factors: (1) processing conditions; (2) blend composition; (3) interface interaction; and (4) viscosity ratio of the components.[7] Controlling the rubber particle size and the size distribution can be achieved by varying the processing conditions and the rubber/resin rheology. The general conclusions are that strong shear fields developed during intense melt extrusion and molding will produce a fine dispersion,[8,9] and a great similarity of apparent viscosity (η_{app}) values of the initial components and low-viscosity rubbers will also result in small particles.[10,11] Simultaneously, the dispersing shape of rubber in the matrix is influenced by the above four factors. There has been some discussion about fibril formation based on the viscosity ratio of the base materials.[12,13] With regard to the viscosity effect on PP/rubber blends, rubber generally disperses in the shape of spherulites in the PP matrix due to the higher viscosity of rubber than that of PP.[11,14–17] However, the effect of the viscosity ratio on the fibril formation in the PP/elastomer system has been sparsely studied.[18,19] In the previous work, fibrillar morphology has been found in the case of both $\eta_d/\eta_m \approx 1$ and $\eta_d/\eta_m > 1$. It implies that fibril formation is probably due to the different interface adhesions be-

Correspondence to: L. Zhang (zlingzi@163.com).
Contract grant sponsors: National Science Foundation; Ministry of Education.

Journal of Applied Polymer Science, Vol. 86, 2085–2092 (2002)

TABLE I
Physical Properties of Base Polymers

Materials	Density (g/cm^3)	MFI (g/10 min)	1-Octent content (wt %)	Producer
PP1	0.90	1.1		1300, Yanshan Chemical (Beijing, China)
PP2	0.91	13		S700, Yangzi Chemical (Nanjing, China)
EOC1	0.87	5	24	8200, DuPont–Dow Chemical (USA)
EOC2	0.863	0.5	28	8180, DuPont–Dow Chemical (USA)
EOC3	0.868	0.5	25	8150, DuPont–Dow Chemical (USA)

PP: MFI under 2.16 kg load at 230°C; EOC: MFI under 2.16 kg at 190°C.

tween the two phases. This article investigated the effect of the interface adhesion combined with the viscosity ratio and the processing conditions on the dispersion of the ethylene–octene copolymer (EOC) domains to PP at a constant composition (75/25). The results provide some understanding of the mechanism of the soft fibril formation and relationship between the morphology and the properties of PP/EOC blends.

EXPERIMENTAL

Materials

The two types of PP and three types of EOC used in the present experiments are listed in Table I.

Processing

To compare with runs a, A, b, and B prepared in the previous work [(a) PP1/EOC1; (A) PP2/EOC1; (b) PP1/EOC2; (B) PP2/EOC2], blends of PP/EOC3 were prepared by melt mixing in a corotating twin-screw extruder (TSSJ-25/32, China) with the same composition of 75/25 and at the same processing conditions. The PP1/EOC2 blend was extruded at 160 rpm and molded at low, medium, and high injection rates to study the effect of the processing conditions on the dispersion (Table II).

Measurements

Rheological properties of the base materials were measured using a capillary rheometer (Kayeness, D5052M) with an L/D of 40 at 190°C.

TABLE II
Formulation of the Blends

	PP1	PP2	EOC2	EOC3
c[a]	75	—	—	25
C[a]	—	75	—	25
b1[b]	75	—	25	—

[a] Screw speed: 120 rpm; injection rate: medium (the same conditions as those used in the previous article).
[b] Screw speed: 160 rpm; injection rates: low, medium, and high.

The interface adhesion of the PP/EOC blends was evaluated by the peel test based on ASTM D 1876-72. In the peel test, the adhesive fracture energy G_a is given by[20]

$$G_a = (\chi - \cos\theta)P \quad (1)$$

where χ is the extension ratio of the flexible member (the elastomer); θ, the peel angle; and P, the peel force per unit width. A 12-mm-wide and 0.3 ± 0.02-mm-thick rubber strip was bonded to two PP films with a thickness of 0.20 ± 0.02 mm at 135°C and 2.0 MPa pressure for 15 min. The measurements were carried out using a tensile tester (AG-10TA, Shimaduz) at a 180° angle at a 50-mm/min rate. The PP film backing restricted the extension of the elastomer strip during the peeling, so that $\chi \approx 1$. The peel force was found to be independent of the elastomer thickness in the ranges tested. A minimum of five strips were examined and the peel force P was evaluated by taking the average. All measurements were conducted at 23°C.

Samples for Izod impact testing were prepared by an injection-molding machine (PS40E5ASE, Nissei) at an injection temperature of 200°C. The impact (GB1843) property of injection-molded samples was investigated using an Izod impact tester (XJU-2.75) at 23°C. At least five runs were made and the results were averaged.

The dispersed morphology of the blends was determined by a scanning electron microscope (X-650, Hitachi). Injection-molded tensile specimens were cryogenically fractured in liquid nitrogen along the flow direction (L direction) and perpendicular to the flow direction (T direction) in the mold. The fractured surfaces were etched in *n*-heptane for 5 min at 50°C and then examined under the SEM.

RESULTS AND DISCUSSION

Effect of viscosity ratio and interface adhesion

The apparent viscosities of the base materials are shown in Figure 1. The viscosity of EOC3 is almost the same as that of EOC2 throughout the shear rate range tested. The viscosity ratio of the PP/EOC3 blends recalculated for the appropriate shear rate ($10^3\ s^{-1}$) at

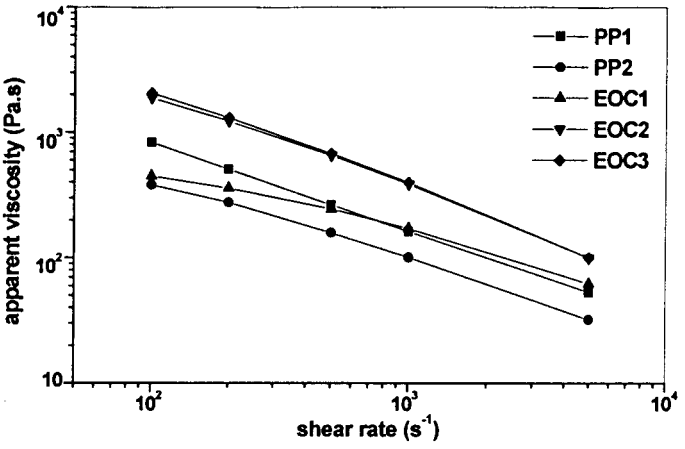

Figure 1 Apparent viscosities of the base materials.

190°C are summarized in Table III. The viscosity ratio of the PP1/EOC3 blend was close to that of the PP1/EOC2 blend (η_d/η_m = 2.40), while the viscosity ratio of PP2/EOC3 was approximately equal to that of the PP2/EOC2 blend (η_d/η_m = 3.84).

Control of the interface adhesion is critical to develop blend morphologies that will yield systems with consistent and acceptable mechanical properties. The interface adhesion for PP against each of the three EOC materials was measured through the peel test. The peel strength P and the adhesive fracture energy G_a between various PPs and EOCs are listed in Table IV. PP1 has better compatibility with EOC than has PP2. Also, the effect of increasing octene content in EOC manifests itself in an increase in the interface adhesion with PP. Higher levels of octene in EOC will thus lead to better compatibility between the two phases, which is consistent with the results revealed by Carriere et al.[21]

Figure 2 shows SEM micrographs of the dispersed morphology of the PP/EOC3 blends. In the transverse direction to flow [Fig. 2(c-T) and (C-T)], EOC3 particles are dispersed in the PP matrix uniformly. In comparing SEM micrographs of the PP/EOC1 and PP/EOC2 blends, which were shown in the previous article,[22] we found that the dispersed diameter of the EOC3 particles in PP is similar to that of EOC2 in PP because the viscosity of EOC3 is close to that of EOC2.

Along the flow direction [Fig. 2(c-L) and (C-L)], short rodlike dispersion of EOC3 is observed. Although the viscosity ratio of the PP1/EOC3 blend is similar to that of the PP1/EOC2 blend, elongated fibrils are hardly found in the PP1/EOC3 system, unlike the short fibrils observed in the PP1/EOC2 system. In the past, various investigators[23,24] pointed out that the major parameter for fibril formation was the viscosity ratio. They reported that if the viscosity ratio was close to unity a uniform thin-thread fibril was formed. They considered the influence of the viscosity ratio only. In fact, the morphology of dispersion is influenced by many factors.[7] As discussed before, interface interaction will also play a great role in the deformation.

In this part of the study, the composition of the blends and the processing conditions are constant. Run a corresponds to $\eta_d/\eta_m \approx 1$; a uniform thin-thread fibril was formed. Runs b and c correspond to $\eta_d/\eta_m > 1$ (η_d/η_m = 2.40 and 2.45, respectively). The fibril formation in PP1/EOC2 is probably due to higher interface adhesion in PP1/EOC2 than in the PP1/EOC3 illustrated above. The viscosity ratio of run A is 1.70, and the interface adhesion of it is the lowest. The formation of coarse and long fibrils in run A may be attributed to good fluidity of EOC1 itself. Thus, it seems to anticipate that a low-viscosity elastomer tends to form fibrils. In Figure 2(C-L), the minor component was dispersed coarsely in spherical, elliptical, and short rodlike domains like run B. When the viscosity of the minor component is too much higher than that of the major one, the viscosity ratio becomes the major parameter determining the dispersing morphology again, because the dispersed phase experi-

TABLE III
Viscosity Ratio of the PP/EOC3 Blends

Run	η_d/η_m
c	2.45
C	3.94

TABLE IV
Peel Strength and Adhesive Fracture Energy of Blends

	Run					
Measurement	a	b	c	A	B	C
P (N/m)	594	1231	945	351	1190	629
G_a(J/m^2)	1188	2462	1890	702	2380	1258

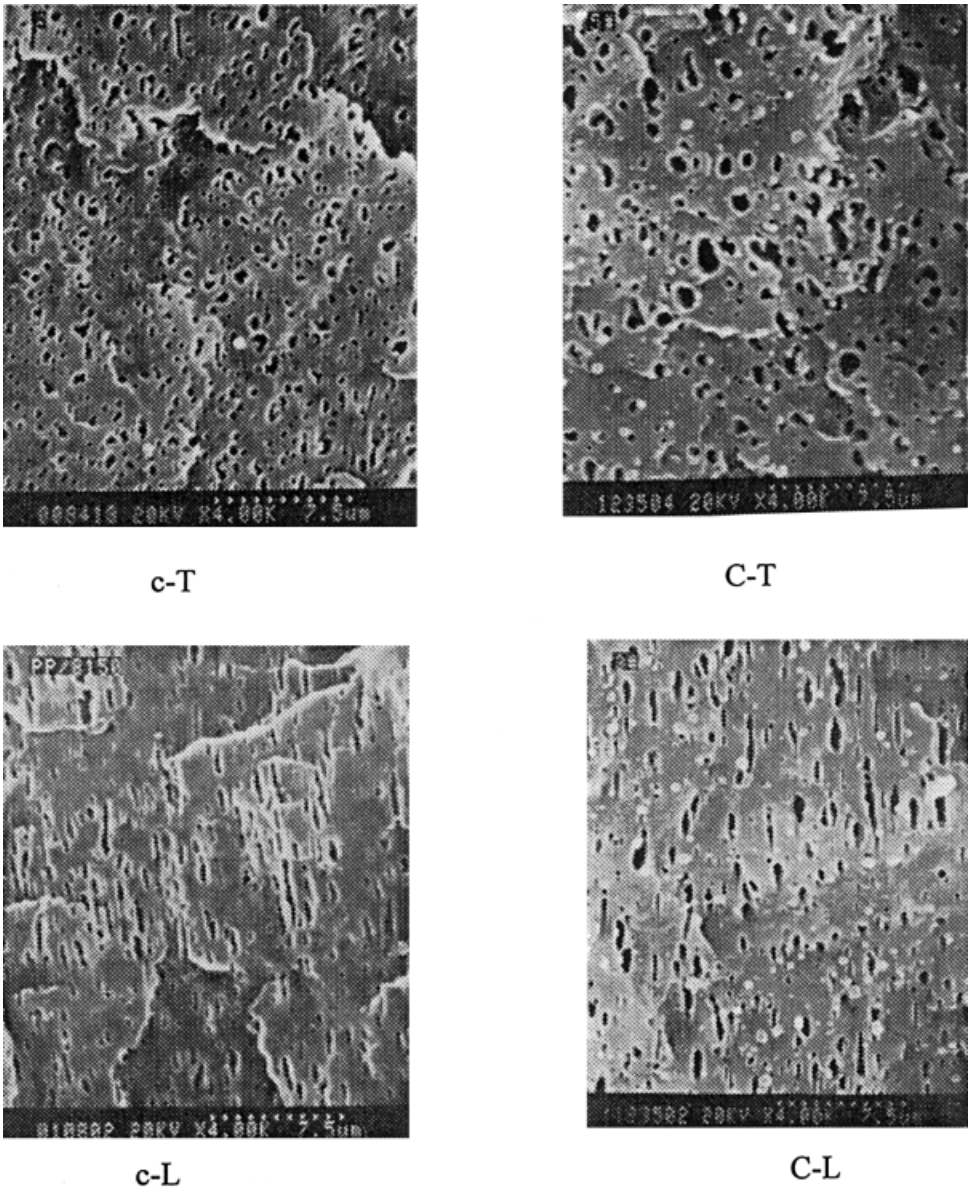

Figure 2 SEM micrographs of the PP/EOC3 blends (T: transverse direction, L: longitudinal direction) c-T, C-T, c-L, and C-L.

ences less deformation than that imposed on the continuous phase and is easy to accumulate.

Figure 3 presents the notched Izod impact strength (I_s) of 25 wt % elastomer-modified PP. The specimens for the impact test were taken from the gate end and far end of the injection-molded bar. The values of I_s obtained for gate-end specimens show systematic deviation toward higher values. Bartczak[25] pointed out that this deviation is caused by some flow-induced orientation present in the injection-molded bar. An impressive jump of the Izod impact strength of PP when modified with the elastomer was observed. Moreover, the samples of plain PP broke completely and were brittle, while the behavior of the samples of the elastomer-modified PP was always of the "non-break" type, except run A, which broke more like plain PP. By taking these observations into account, one can conclude that the relative toughness of elastomer-modified PP to that of plain PP is even higher than that shown in Figure 3.

Figures 4 and 5 shows the dependence of the relative toughness ($\beta = I_{sb}/I_{sm}$, subscripts b and m designate the blend and the matrix, respectively) on the viscosity ratio and the interface adhesion, respectively. In these figures, β of run a with fine fibrils is higher than that of run A with coarse fibrils, indicating that, for a similar dispersing morphology, I_s increases with decrease of the viscosity ratio, namely, the decrease of the dispersing size and the increase of the interface adhesion. Figure 5 shows that I_s increased with an increasing interface adhesion in the same matrix. Run A, having a weak adhesion of $G_a = 702$ J/m^2, is brittle.

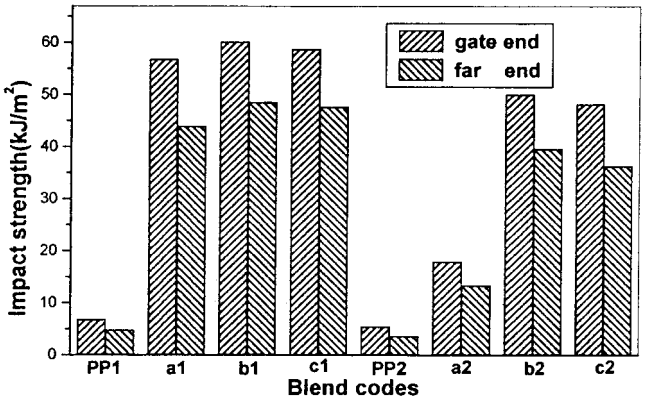

Figure 3 Notched Izod impact strength for all blends.

Thus, the adhesion of G_a = 702 J/m^2 is too low for toughening on impact. The other blends showed a fracture surface with large plastic deformation and whitening.

The small disparity of the impact strengths of runs a, b, and c suggests that the minimum adhesion required for toughening should be between 702 and 1188 J/m^2. The minimum adhesion required should be about equal to the tear energy of the elastomer to ensure that the elastomer particles are not detached from the matrix during fracture. A typical lower limit of elastomer tear energy[26] is about 1000 J/m^2. We thus suggest that the minimum adhesion required for toughening should be about 1000 J/m^2. Stronger adhesion above this level alone is not sufficient for toughening. In comparing runs b and B, short fibril formation in run b results in a lower β than in run B with spherical, elliptical, and short rodlike dispersion, indicating that soft fibril formation suppresses improvement of the impact strength. Hence, one can expect that the toughness of elastomer-modified PP depends on the dispersed morphology determined by the viscosity ratio and the interface adhesion.

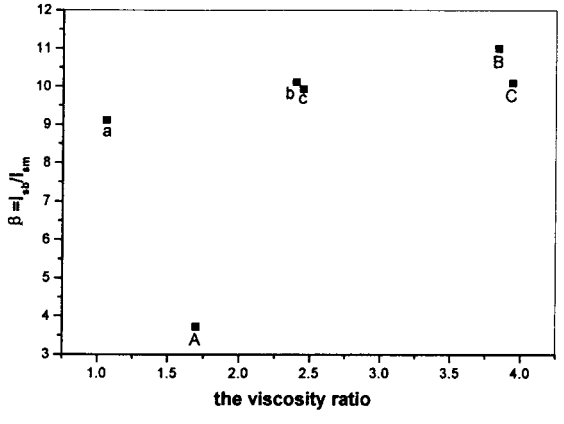

Figure 4 Relative toughness β as a function of the viscosity ratio.

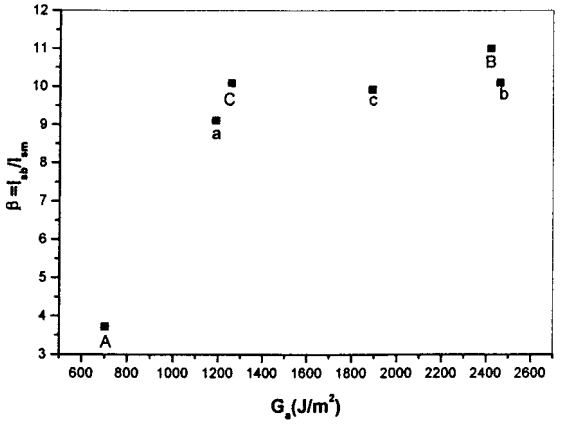

Figure 5 Relative toughness β as a function of the adhesive fracture energy G_a.

Effect of processing conditions

It can be seen in the preceding paragraphs (on the effect of interface adhesion and the viscosity ratio on dispersion) that blend PP1/EOC2, having the highest interface adhesion and $\eta_d/\eta_m > 1.0$, produced short fibrillar dispersion. The fibrillar dispersion apparently resulted from the high interface adhesion. This same system was chosen to study the influence of processing conditions, namely, whether variations in processing shear histories would affect the dispersion behavior of EOC2 in PP1.

Two screw speeds (120 and 160 rpm) were employed in this work to provide "low" and "high" mixing shear, respectively. A high screw speed generates a high mixing shear. Although the mixing time at a high screw speed is less than that at a low screw speed, this difference seems to be negligible because the screw length is low. Figure 6 shows T-direction SEM micrographs of the PP1/EOC2 blend prepared at 120 rpm (run b) and 160 rpm (run b1), respectively. To provide a quantitative assessment of the effect of the extrusion condition on the dispersion, representative elastomer particles were measured and counted using SEM micrographs at magnifications from 3000× to 10,000×. The results are presented in Figure 7. Three parameters—namely, the number (D_n)- and weight (D_w)-average size and the size distribution (D_w/D_n) are important descriptors of the dispersion. A comparison of these parameters in Figure 7 assumes that D_n decreases from 0.25 to 0.19 μm, with an increasing screw speed from 120 to 160 rpm, contributing a slight improvement of toughness from 60.1 to 62.0 kJ/m^2. The L-direction SEM micrograph of the PP1/EOC2 blend prepared at 160 rpm is illustrated in Figure 8(b), which is similar to that of the PP1/EOC2 blend prepared at 120 rpm.[22] It seems that a high shear rate in extrusion has no effect on fibrillar formation.

When the blend is flowing, the deformation and the consequent breakdown of the dispersed domains are

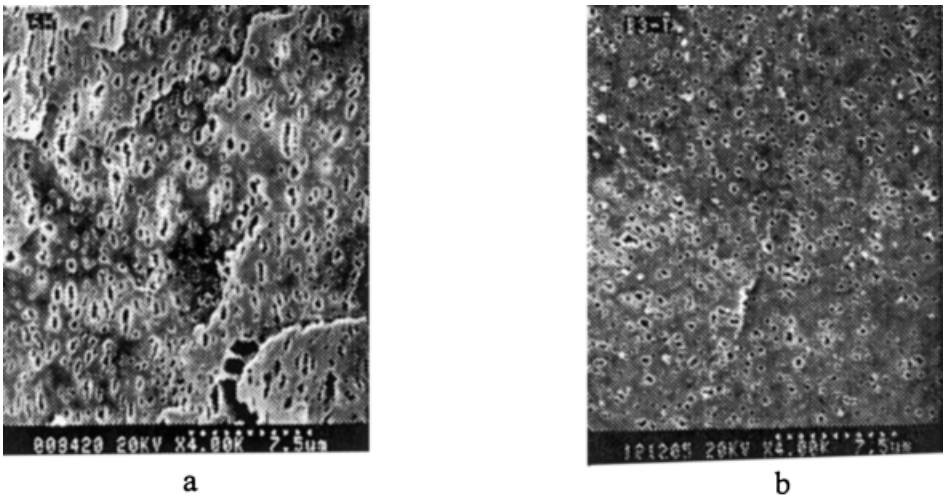

Figure 6 T-direction SEM micrographs of the PP1/EOC2 blend at different screw speeds: (a) 120 rpm; (b) 160 rpm.

accompanied by a competitive process of coalescence. Figure 8 shows the L-direction SEM micrographs of the PP1/EOC2 blend at different injection rates. In Figure 8(a), EOC2 disperses nonuniformly in the matrix at a low injection rate. We observed many irregular large particles, indicating that particle coalescence

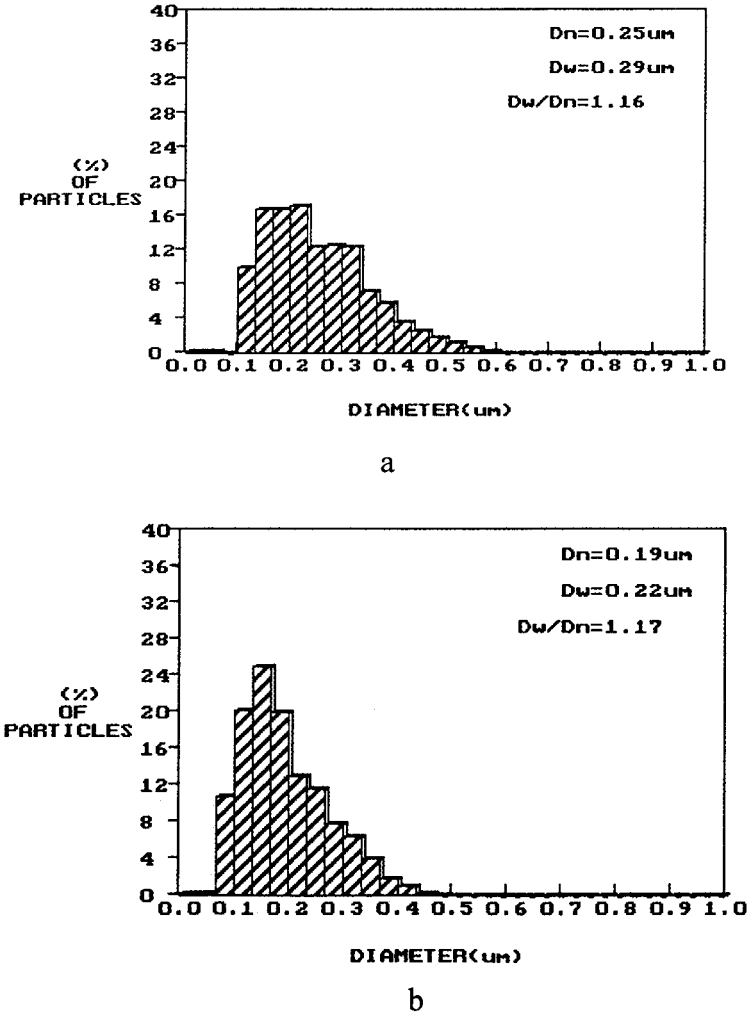

Figure 7 Particle-size distribution versus processing conditions in PP1/EOC2 blend: (a) 120 rpm; (b) 160 rpm.

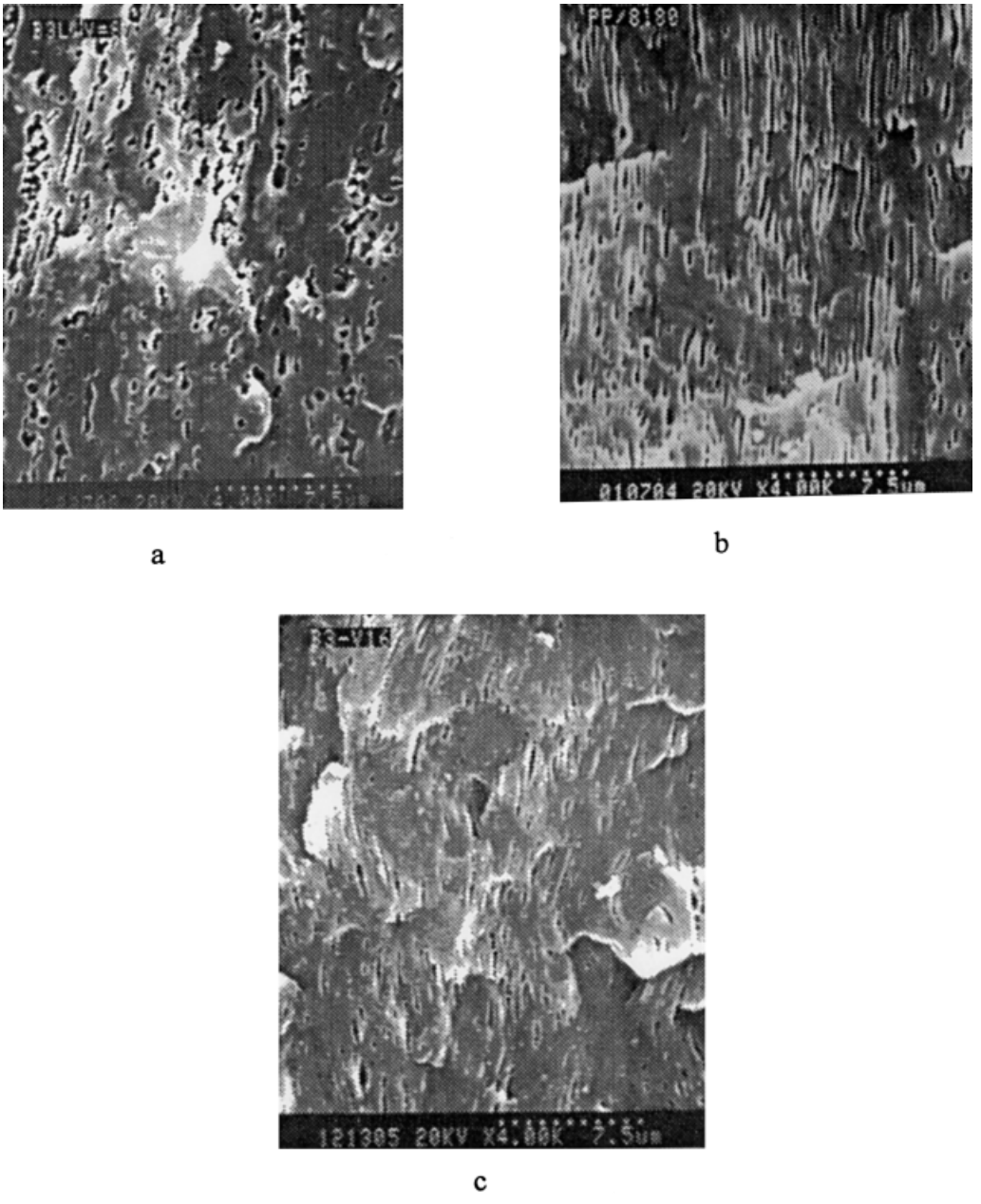

Figure 8 L-direction SEM micrographs of the PP1/EOC2 blend at different injection rates: (a) low; (b) medium; (c) high.

occurs at a low injection shear rate. At the medium injection rate, the deformation process of the dispersed component becomes predominant and brings about fine and uniform structures elongated in the flow direction [Fig. 8(b)]. As the injection rate increases further, the higher values of shear stress and the turbulence of the stream facilitate the breakdown process of the dispersed elements oriented in the flow direction.[27,28] The morphological consequence is an overall reduction in the state of orientation of the dispersed domains.

Table V lists the notched Izod impact strength of run b1 at different injection rates. The toughness increase with an increasing injection rate can be interpreted by the fine and uniform dispersion and breakdown of oriented fibrils at a high injection rate.

TABLE V
Impact Strength of PP1/EOC2 Blend at Different Injection Rates

Injection rate	Impact strength (kJ/m^2)
b1 at low	59.5
b1 at medium	62.0
b1 at high	64.2

CONCLUSIONS

A reasonable explanation of the microstructure in PP/EOC blends has been developed in terms of the viscosity ratio, the interface interaction, and processing conditions. For the same processing history, fibril formation was related to both the viscosity ratio and the interface adhesion. A close to unity viscosity ratio and a high interface adhesion resulted in fibril dispersion. A low-viscosity elastomer tended also to form fibrils.

A high shear rate in extrusion seems to have no effect on fibrillar formation, but the dispersion size (D_n) decreased from 0.25 to 0.19 μm with an increasing screw speed from 120 to 160 rpm. In the molding flow, there exists a competitive process between the deformation and the consequent breakdown and coalescence of the dispersed domains. Nonuniform and large particles were obtained at a low injection rate due to coalescence. At the medium injection rate, the deformation process of the dispersed component became predominant and brought about fine and uniform short fibrils elongated in the flow direction. A high injection rate facilitated the breakdown process of the dispersed elements oriented in the flow direction.

The toughness of elastomer-modified PP is influenced mainly by the dispersed morphology determined by the viscosity ratio, the interface adhesion, and processing conditions. The minimum adhesion required for toughening is proposed to be about 1000 kJ/m^2. Stronger adhesion above this level alone is not sufficient for toughening. The Izod impact strength of the blends appears to be optimum when a fine, uniform, and nonfibril morphology of the elastomer in PP is formed.

The authors gratefully acknowledge the National Science Foundation as well as the Ministry of Education Foundation for financial support. The authors extend their gratitude to Dr. Li Zhongming for helpful discussion.

References

1. Michler, G. H.; Starke, J.-U. In Toughened Plastics II: Science and Engineering; Riew, C. K.; Kinloch, A. J., Eds.; American Chemical Society: Washington, DC, 1996; p 251.
2. D'Orazio, L.; Mancarella, C.; Martuscelli, E., et al. Polymer 1999, 40, 2745.
3. Choudhary, V.; Varma, H. S.; Varma, I. K. Polymer 1991, 32, 2534.
4. Yamaguchi, M.; Suzuki, K.; Miyata, H. J. Polym Sci Polym Phys 1999, 37, 701.
5. Gupta, A. K.; Purwar, S. N. J Appl Polym Sci 1984, 29, 1595.
6. Gupta, A. K.; Purwar, S. N. J Appl Polym Sci 1985, 30, 1777.
7. Kuleznev, V. N. Blends of Polymers; Khimiya: Moscow, 1980.
8. Speri, W. M.; Patrick, G. R. Polym Eng Sci 1975, 15, 668.
9. Han, C. D.; Villamizar, C. A.; Kim, Y. M. J Appl Polym Sci 1977, 21, 351.
10. Wu, S. Polym Eng Sci 1987, 27, 335.
11. Baranov, A. O.; Medintseva, T. I.; Zhorina, L. A. et al. J Appl Polym Sci 1999, 73, 1563.
12. Tsebrenko, M. V.; Rezanova, N. M. Polym Eng Sci 1980, 20, 1023.
13. Min, K.; White, J. L. Polym Eng Sci 1984, 24, 1327.
14. Kim, B. K.; Do, I. H. J Appl Polym Sci 1996, 61, 439.
15. Danesi, S.; Porter, R. S. Polymer 1978, 19, 448.
16. Van der Wal, A.; Nijhot, R.; Gaymans, R. J. Polymer 1999, 40, 6031.
17. Dao, K. C. Polymer 1984, 25, 1527.
18. Kim, B. K.; Do, I. H. J Appl Polym Sci 1996, 60, 2207.
19. Kim, B. K.; Kim, M. S.; Kim, K. J. J Appl Polym Sci 1993, 48, 1271.
20. Wu, S. Polymer Interface and Adhesion; Marcel Dekker: New York, 1982.
21. Carriere, C. J.; Silvis, H. C. J Appl Polym Sci 1997, 66, 1175.
22. Zhang, L.; Huang, R.; Li, L. B. J Appl Polym Sci 2002, 83, 1870.
23. Cox, R. G. J Fluid Mech 1969, 37, 601.
24. Tomotika, S.; Cox, R.; Mason, S. G. J Colloid Sci 1972, 38, 395.
25. Bartczak, Z.; Argon, A. S.; Cohen, R. E., et al. Polymer 1999, 40, 2347.
26. Wu, S. Polymer 1985, 26, 1855.
27. White, J. L.; Ufford, R. C.; Dharod, K. R.; Price, R. L. J Appl Polym Sci 1973, 16, 1313.
28. Albanova, T. I.; Tsebrenko, M. B.; Yudin, A. B. V.; Vinogradov, G. V.; Yarbykov, B. V. J Appl Polym Sci 1975, 19, 1781.